Molecular Crystals and Liquid Crystals

Publication details, including instructions for authors and subscription information:
http://www.tandfonline.com/loi/gmcl20

THREE-DIMENSIONAL NUMERICAL SIMULATION FOR UNDERSTANDING THE FRINGE-FIELD EFFECT ON THE DYNAMIC BEHAVIOR OF LIQUID CRYSTAL

Sang-Ho Yoon [a b], Cheol-Soo Lee [a b], Suk-In Yoon [a b], Jun-Hee Lee [a b], Hyung-Jin Yoon [a b], Min-Wan Choi [a b], Jin-Woo Kim [a b] & Taeyoung Won [a b]

[a] Department of Electrical Engineering, School of Engineering, Inha University, 253 Yonghyun-Dong, Nam-Gu, Incheon 402-751, Korea

[b] Sanayi System Co., Ltd., 1505 SWEN Daelim Building, 592-5 Dohwa-Dong, Nam-Gu, Incheon 402-711, Korea

Version of record first published: 07 Jan 2010

To cite this article: Sang-Ho Yoon, Cheol-Soo Lee, Suk-In Yoon, Jun-Hee Lee, Hyung-Jin Yoon, Min-Wan Choi, Jin-Woo Kim & Taeyoung Won (2004): THREE-DIMENSIONAL NUMERICAL SIMULATION FOR UNDERSTANDING THE FRINGE-FIELD EFFECT ON THE DYNAMIC BEHAVIOR OF LIQUID CRYSTAL, Molecular Crystals and Liquid Crystals, 413:1, 333-343

To link to this article: http://dx.doi.org/10.1080/15421400490437033

Mol. Cryst. Liq. Cryst., Vol. 413, pp. 333/[2469]–343/[2479], 2004

ISSN: 1542-1406 print/1563-5287 online
DOI: 10.1080/15421400490437033

THREE-DIMENSIONAL NUMERICAL SIMULATION FOR UNDERSTANDING THE FRINGE-FIELD EFFECT ON THE DYNAMIC BEHAVIOR OF LIQUID CRYSTAL

Sang-Ho Yoon, Cheol-Soo Lee, Suk-In Yoon, Jun-Hee Lee, Hyung-Jin Yoon, Min-Wan Choi, Jin-Woo Kim, and Taeyoung Won
Department of Electrical Engineering, School of Engineering, Inha University, 253 Yonghyun-Dong, Nam-Gu, Incheon 402-751, Korea
and
Sanayi System Co., Ltd., 1505 SWEN Daelim Building, 592-5 Dohwa-Dong, Nam-Gu, Incheon 402-711, Korea

A three-dimensional numerical study for understanding the fringe-field effect on the dynamic behavior of liquid crystal is presented. Our three-dimensional numerical simulator (TechWiz LCD) is based on the FEM (finite element method) formulation of Ericksen-Leslie equation, flow equation, and Laplace equation. Since our FEM solver has a fully unstructured mesh generator, it is possible to investigate the dynamic performance of any mode of LC cell with an arbitrarily shaped electrode structure including a chevron-type LC cell. In this paper, we report our preliminary result on the simulation of the dynamic behavior of the fringe-filed switching (FFS) mode LC cell that is designed for the fast response and wide viewing angle. The simulated dynamic response of the director distribution for the FFS-mode LC cell is also compared with experimental observations. The simulation reveals that most of the directors over the LC cell experience horizontal rotations despite the existence of both the vertical and the horizontal electric fields in the LC cell.

Keywords: finite element method; liquid crystal display; simulation

This work has been partly supported by the Ministry of Information & Communication of Korea (Support Project of University Information Technology Research Center Program supervised by KIPA) and partly by the Ministry of Science and Technology through KISTEP.

INTRODUCTION

In order to improve the optical performances of an LCD panel such as a viewing angle and a response time, a great deal of research efforts have been made on the development of novel modes of LC cell with an arbitrarily shaped electrode structure such as an in-plane switching (IPS) mode, a fringe-field switching (FFS) mode, a patterned vertical alignment (PVA) mode, and a multi-domain vertical alignment (MVA) mode [1]. The electrode structure of the above-mentioned devices has a complexity when compared with that of the traditional TN-LCD. As a consequence, it is necessary to conduct a multi-dimensional modeling of liquid crystal cell for the optimization of the high-performance display panel with advanced modes of operation. In this work, an FFS-mode LC cell having inter-digitated electrodes was investigated in an effort to understand the fringe-field effect on the dynamic behavior of directors of an LC cell with our three-dimensional FEM simulator (TechWiz LCD) [2].

Many researchers have proposed several numerical models for characterizing the dynamics of liquid crystal, which is based on the Frank-Oseen free energy density model [3–5]. Furthermore, various numerical techniques have been applied in order to solve the equations, which are quite nonlinear, describing the hydrodynamic motions of liquid crystal [6]. Several models for the liquid crystal cell were developed for dealing with pure nematic, twisted nematic, and cholesteric liquid crystal materials. Two popular approaches for numerical calculation of the above-mentioned governing equations are finite difference method and finite element method. Since it is difficult to obtain an accurate solution from the finite difference method for the chevron-type structures of liquid crystal cell (e.g. IPS, MVA, FFS etc.) due to a geometric complexity, a finite element method has been used in order to ensure flexibility in the design of the liquid crystal cell.

NUMERICAL MODEL

According to the continuum theory of Ericksen and Leslie [7], the equation of motion for nematic liquid crystal is given by

$$\gamma_1 \dot{\boldsymbol{n}}_i = \gamma n_i - \frac{\partial F}{\partial n_i} - \gamma_1 N_i - \gamma_2 n_j A_{ij} + \left(\frac{\partial F}{\partial n_{i,j}}\right)_{,j} \tag{1}$$

where F is the free energy density, γ_1 is the rotational viscosity ($\alpha_3 - \alpha_2$), $\gamma_2 = \alpha_3 + \alpha_2$, γ is the Lagrange multiplier, $A_{ij} = (v_{i,j} + v_{j,i})/2$, $N_i = \dot{\boldsymbol{n}}_i + (v_{i,j} + v_{j,i})n_j/2$, and n_i denotes the director with $|n_i| = 1$ and (i, $j = x$, y, z). The free-energy density F^B in the bulk is taken in the form of the Frank-Oseen energy.

$$F^B = \frac{1}{2}k_{11}(\mathrm{div}\,\vec{n})^2 + \frac{1}{2}k_{22}(\vec{n}\cdot curl\,\vec{n})^2 + \frac{1}{2}k_{33}(\vec{n}\times curl\,\vec{n})^2 + \frac{2\pi}{p_0}k_{22}(\vec{n}\cdot curl\,\vec{n}) - \frac{1}{2}\varepsilon_0 grad\,V\cdot\varepsilon\cdot grad\,V \quad (2)$$

where $\vec{n}$ denotes the director, V denotes the electric potential, k_{11}, k_{22}, and k_{33} are Frank's elastic constants and p_0 is the natural pitch. The dielectric anisotropy of the liquid crystal is described by the uniaxial tensor,

$$\varepsilon = \varepsilon_\perp\delta_{ij} + \left(\varepsilon_\parallel - \varepsilon_\perp\right)n_i n_j \quad (3)$$

where $\varepsilon_\parallel$ and $\varepsilon_\perp$ are the dielectric constants for parallel and perpendicular orientation of the director relative to the electric field. The Ericksen-Leslie equations for the director field are obtained from the condition of the stationary total energy F, which leads to separate bulk and surface equation.

It is well known that the dynamic analysis of liquid crystal is important for the estimation of LCD performance. There exist several numerical techniques for updating the director distribution for every time step (defined by continuum model of the liquid crystal) such as the successive displacement approach or the simultaneous displacement algorithm. Successive displacement algorithm contains inevitable numerical errors during the successive iteration for each grid point from the solutions of the surrounding grid points. Consequently, the simultaneous displacement algorithm has been chosen for rigorous multi-dimensional FEM simulation. Furthermore, an explicit scheme has been employed in the transient calculation to resolve the strong non-linearity of the governing equation. In each time-step, the FEM code solves Laplace equation for electric potential distribution in response to the applied potential, which in turn affects the director distribution.

The Ericksen-Leslie equation constitutes a set of coupled nonlinear partial differential equations, which are to be solved numerically. Because of the strong non-linearity of the Ericksen-Leslie equation, the numerical procedure is very tricky. The numerical procedure under consideration comprises two steps of iterative treatment. Firstly, we obtained the solution for voltage by Laplace equation, given a known director distribution. Thereafter, the Ericksen-Leslie equation is solved for estimating the director deformation when the distribution of voltage is known. Dirichlet boundary conditions were applied on the surface of the liquid crystal in the Ericksen-Leslie equation and the surface of the electrode in the Laplace equation solver. Repeating the above steps for each time-step leads us to the solutions.

The Ericksen-Leslie equation is formulated via Galerkin method, while the Laplace equation is formulated via Ritz method for the finite element calculation. The liquid crystal cell is discretized with linear tetrahedron mesh elements using the advancing front algorithm [8]. The normalization of the director is performed for each time step, and the cell capacitance is extracted from the energy method [9].

SIMULATION AND DISCUSSIONS

As a first step, a multi-layer mask structure (GDS-II format) is drawn using our layout editor, as shown in Figure 1(a), followed by a process of defining a three-dimensional structure of LC cell from the process recipe. Inter-digital pixel electrode is located on the common electrode. Whole electrodes are defined in the lower region of the LC cell. A three-dimensional tetrahedral mesh is generated for the LC cell as shown in Figure 1(b).

Thereafter, a three-dimensional structure is sequentially generated from the process information for each mask layer, as shown in Figure 2. Common electrode and gate bus lines are generated from the mask layout, as depicted in Figure 2(a). Pixel electrode and data electrode are also generated above the oxide layer overlying the common electrode and the gate

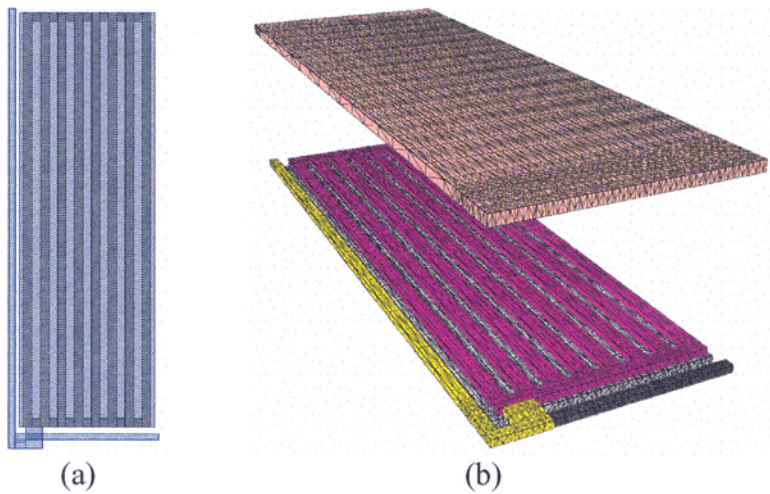

FIGURE 1 A schematic diagram illustrating the steps of generating an arbitrarily shaped electrode structure from the GDS-II mask layout: (a) mask layout for the FFS mode LC cell, and (b) mesh generation for the LC cell automatically constructed from the process recipe. (See COLOR PLATE XVII)

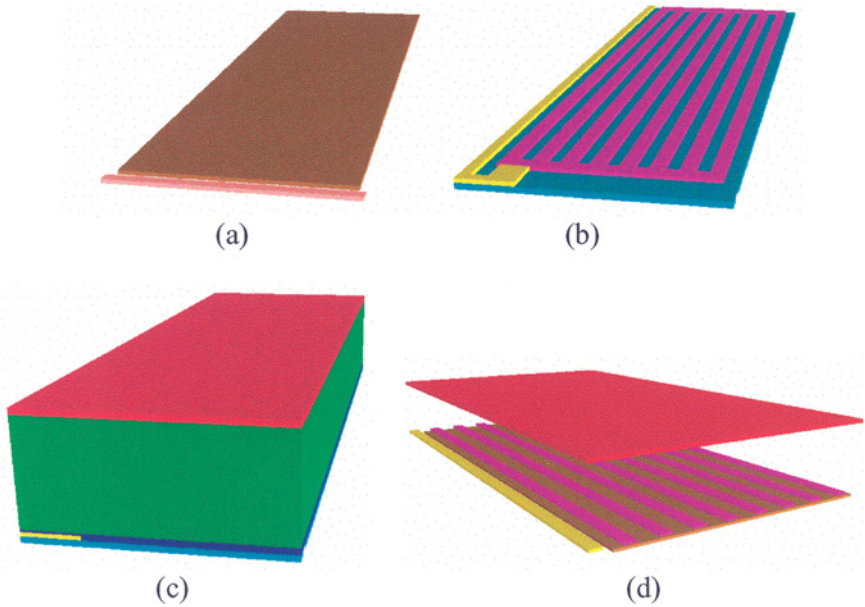

FIGURE 2 A schematic diagram illustrating the workflow for the structure generation from the mask layout: (a) common electrode and gate electrode, (b) pixel electrode and data electrode, (c) oxide layer, liquid crystal, and the glass regions, (d) extraction of the simulated region. (See COLOR PLATE XVIII)

line, as shown in Figure 2(b). The oxide layer, the liquid crystal, and the glass layer are sequentially generated, as shown in Figure 2(c). Figure 2(d) shows a structure partially bisected from the LC cell for the computational efficiency during the simulation. Figure 2 is a schematic diagram illustrating the expanded views along the z-direction.

The calculations are performed for the liquid crystal material that is characterized by elastic parameters $k_{11} = 13.2\,pN$, $k_{22} = 6.5\,pN$, $k_{33} = 18.3\,pN$, dielectric constants $\varepsilon_{\|} = 8.3$, $\varepsilon_{\perp} = 3.1$, rotational viscosity $\gamma_1 = 123.2\,mPa \cdot s$, refractive indices $\mathrm{n_e} = 1.5763$, $\mathrm{n_o} = 1.4794$; a cell gap of 5 micron, 1° pre-tilt angle, 88° azimuthal angle, and natural pitch of 100 micron. In Figure 3 are shown the plots illustrating the simulation results for the FFS mode LC cell, which include an electric potential distribution, a director distribution at a cross-sectional plane including the center of the cell gap, and optical transmission. As shown in Figure 3, a relatively low transmission is observed at the open area of the pixel electrode. The pixel electrode region, however, has a relatively high transmission. Since this seems to be due to a numerical error from the shortage of the number of calculating points, a mesh refinement is needed

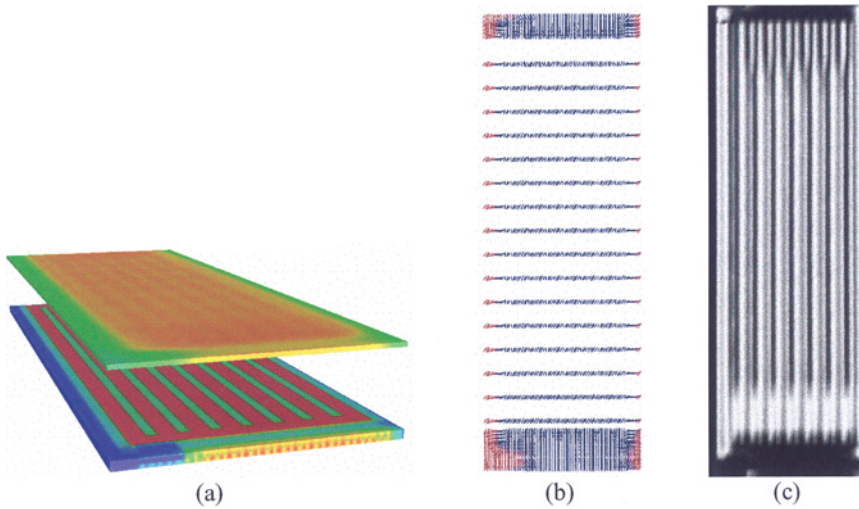

FIGURE 3 Plots showing the simulation results for the FFS mode LC cell: (a) electric potential distribution, (b) director distribution at a cross-sectional plane along a center of the cell gap, (c) optical transmission. (See COLOR PLATE XIX)

as depicted in Figure 4. Figure 4 illustrates the mesh generated for refinement and a recalculated electric potential distribution. Horizontal electric fields are generated between the pixel electrode and the common electrode, while the vertical electric fields are also generated on the electrodes. It should be noted that the vertical behavior is observed on the electrode while the horizontal behavior is observed between the electrodes due to the distribution of the electric fields. However, it is well known that only the horizontal behavior is observed in the FFS mode LC cell.

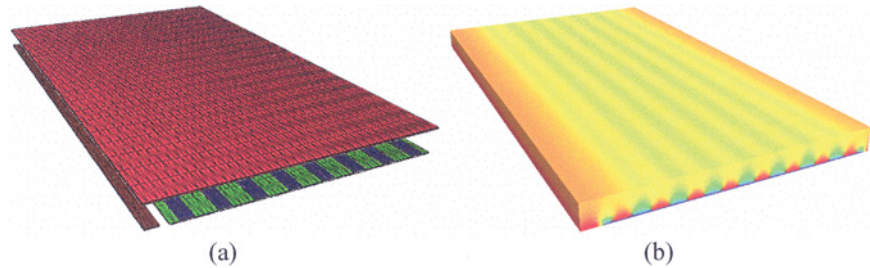

FIGURE 4 Plots illustrating the simulation results for an partial region of the LC cell: (a) mesh structure, (b) distribution of electric potential. (See COLOR PLATE XX)

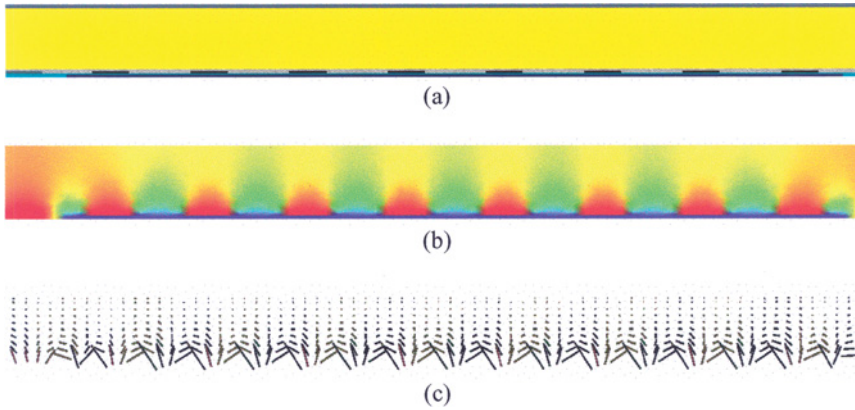

FIGURE 5 A cross-sectional view: (a) cross-sectional view of the LC cell, (b) distribution of electric potential, and (c) distribution of electric field. (See COLOR PLATE XXI)

The director distribution was calculated for the LC cell using finite element method. Furthermore, the transient simulation was carried out for the analysis of dynamic characteristics. Cross-sectional views of the simulation result are depicted in Figure 5. Figure 5(a) shows the cross-sectional view of the LC cell with width of 3 microns and with a gap of 5 microns of pixel electrode. Figure 5(b) and (c) show the distribution of electric potential and electric field, respectively. As shown in the figures, the vectors of the electric field are aligned vertically around the pixel electrode.

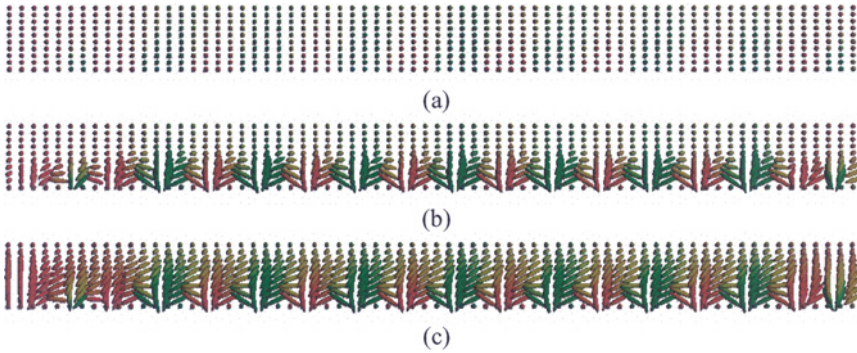

FIGURE 6 Cross-sectional views of director distribution at (a) time = 0 msec, (b) time = 10 msec, and (c) time = 50 msec. (See COLOR PLATE XXII)

Figure 6(a) shows the distribution of the initial directors. All of the directors are set up with a pre-tilt angle of 1° and an azimuthal angle of 88° at the beginning. Directors are rotated horizontally between electrodes after 10 msec, as shown in Figure 6(b). High electric field, which was 3.5×10^6 V/m in the x direction, has been generated between the electrodes. The magnitude of electric field in other regions of liquid crystal cell was a few of 10^5 V/m. Therefore, directors located in the region under the high electric field are rotated prior to the others at the early stage of deformation. Figure 6(c) shows the simulated director deformation after 50 msec. This figure demonstrates the occurrence of horizontal deformation in the whole region of the liquid crystal cell. Furthermore, directors in the region under the vertical electric field have been rotated horizontally.

It can be figured out that the horizontal deformation in the region under the vertical electric field should not be influenced by the electric field. Vertical electric field is applied on the electrode while the horizontal electric field is generated between electrodes. However, it should be noted that the strength of the horizontal field is stronger than that of the vertical field, as depicted in Figure 5(c). The calculated magnitudes of the electric field are 3.9×10^6 V/m between the pixel electrode and common electrode, while 9.8×10^5 V/m on the pixel electrode, 2.7×10^6 V/m on the common electrode, and a few 10^5 V/m in the upper region of the liquid crystal cell. The direction of the electric fields at the center of each electrode is aligned to the z-direction. Therefore, the deformation of directors cannot be explained entirely by electric field distributions.

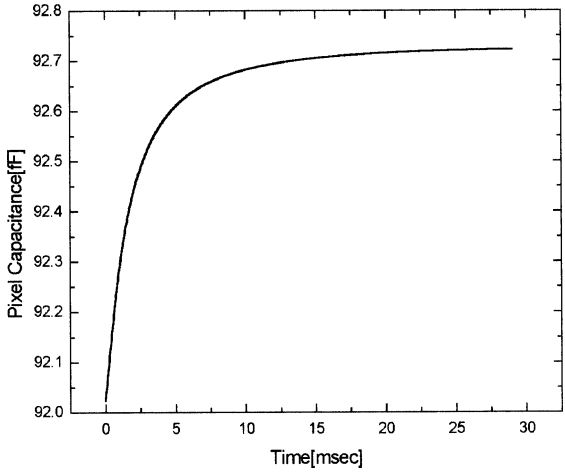

FIGURE 7 A plot showing the simulated cell capacitance as a function of time.

Furthermore, the transient variation of the cell capacitance has been investigated for understanding the relationship between the director distribution and the electric field distribution, as shown in Figure 7. Cell capacitance between the pixel electrode and the common electrode keeps increasing by the moment of 10 msec, while the cell capacitance being saturated beyond that point. This implies that the deformation of directors after the moment of 10 msec is not influenced by the distribution of electric fields.

The dynamic analysis reveals that directors in the lateral region of electrodes tend to respond more rapidly and are thereafter slowly rotated at the upper region of electrode. Furthermore, it is revealed that the cell capacitance is saturated in less than 10 msec. Consequently, it seems that the directors are independent of the electric field distribution after the saturation of cell capacitance, which is due to the relative interaction between adjacent directors. Directors in a strong lateral electric field region are rotated by the electric field beforehand, and then directors in the upper electrode region are rotated slowly by the distribution of neighboring directors.

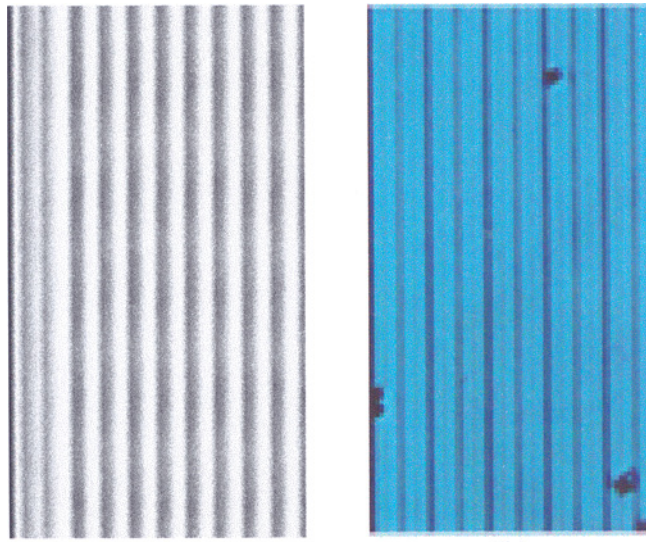

FIGURE 8 Comparison of simulation and experiment for the optical characteristics of the FFS mode LC cell: (a) simulated transmittance distribution for the extended structure of the LC cell, and (b) photo of real LC cell [2]. (See COLOR PLATE XXIII)

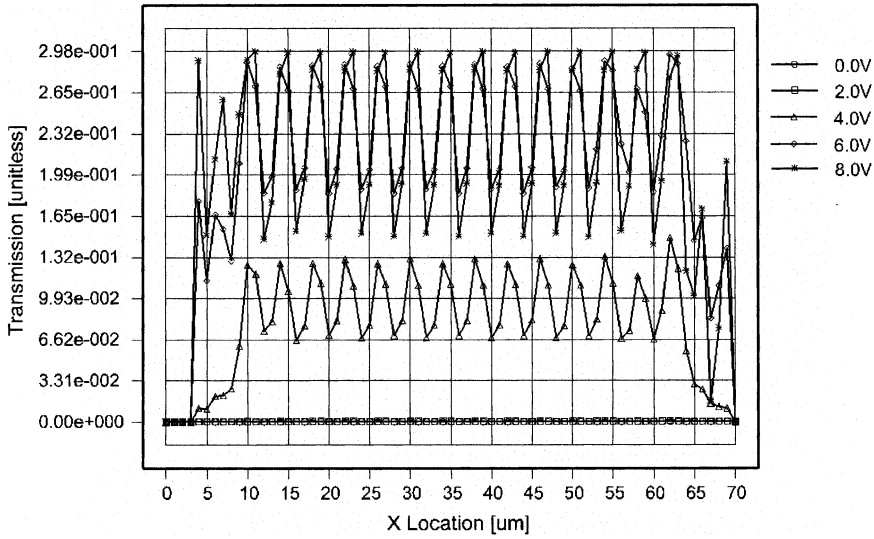

FIGURE 9 Calculated optical transmission along the horizontal direction of the cell with varying the pixel voltage.

Figure 8 shows the simulation result with a photo exhibiting the optical transmittance for the liquid crystal cell. In Figure 8(a) is shown the simulated transmittance distribution for the liquid crystal cell by the extended Jones's method [10]. The transmittance is varied in the regions on the pixel electrode or common electrode. This is due to the fact that the directors are tilted up near the electrode edges. The comparison between the simulation result and experimental transmittance demonstrates an excellent coincidence, as shown in Figure 8(a) and Figure 8(b). Figure 9 shows the distribution of transmission along the horizontal direction of the cell for the pixel voltage.

CONCLUSION

Dynamic behavior of FFS mode liquid crystal cell has been investigated using our three-dimensional FEM simulator (TechWiz LCD). Theoretical explanations were made on the horizontal rotation over the liquid crystal cell from transient analysis of director and cell capacitance. Even with the fringe fields generated over the LC cell for the FFS mode, strong horizontal fields tend to be generated in the lateral region of the electrode, while vertical fields are generated on the electrode. The transient simulation reveals that directors in the lateral region of electrodes respond more

rapidly and thereafter are slowly rotated at the upper region of electrode. Furthermore, the transient simulation reveals that the cell capacitance is saturated in less than 10 msec. Consequently, it seems that the directors are independent of the electric field distribution after the saturation of cell capacitance, which is due to the relative interaction between the adjacent directors. Directors in a strong lateral electric field region are rotated by the electric field beforehand, and then directors in the upper electrode region are rotated slowly by the distribution of the neighboring directors. The transient characteristics of LC cell have also been confirmed by the electric field and the elastic energy of FFS mode LC cell.

REFERENCES

[1] Lee, S. H. & Lee, M.-H. (2001). *J. Korean Phys. Soc.*, *39*, S42.
[2] TechwizLCD databook, http://www.sanayisystem.co.kr.
[3] Dickmann, S., Eschler, J., Cossalter, O., & Mlynski, D. A. (1993). *Digest of Tech. Papers of SID Intl. Symposium*, 638.
[4] Chen, C.-J., Lien, A., & Nathan, M. I. (1995). *Digest of Tech. Papers of SID Intl. Symposium*, 548.
[5] Mori, H., Gartland, E. C., Kelly, J. R., & Bos, P. J. (1999). *Jpn. J. Appl. Phys.*, *38*, 135.
[6] Anderson, J. E., Titus, C., Watson, P., & Bos, P. J. (2000). *Digest of Tech. Papers of SID Intl. Symposium*, 35.4.
[7] Chandrasekhar, S. (1992). *Liquid crystals*, Cambridge University Press: Cambridge, Chap. 3.
[8] Yoon, S., Lee, J., Yoon, S., Kwon, O., & Won, T. (2000). *IEICE Trans. on Electron.*, *E83-c*, 1349.
[9] Yoon, S., Kwon, O., & Won, T. (2001). *J. Korean Phys. Soc.*, *39*, 87.
[10] Berreman, D. W. (1972). *J. Opt. Soc. America*, *62*, 502.